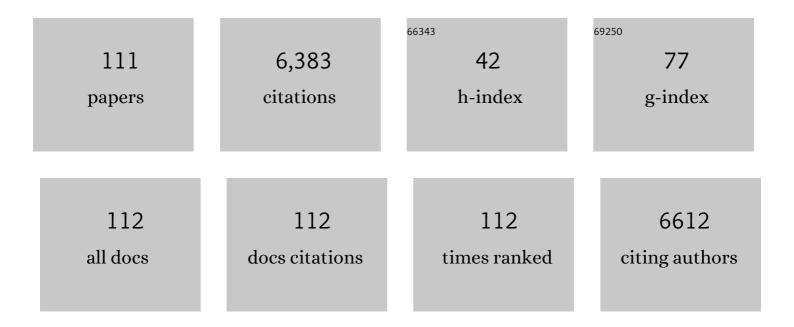
List of Publications by Year in descending order

Source: https://exaly.com/author-pdf/1517628/publications.pdf Version: 2024-02-01



MIN CHEN

| #  | Article   | IF   | CITATIONS |
|----|---|------|-----------|
| 1  | Iron and chromium co-doped cobalt phosphide porous nanosheets as robust bifunctional electrocatalyst for efficient water splitting. Nanotechnology, 2022, 33, 075204.   | 2.6  | 9         |
| 2  | Interfacing Co3Mo with CoMoOx for synergistically boosting electrocatalytic hydrogen and oxygen evolution reactions. Chemical Engineering Journal, 2022, 431, 133240.   | 12.7 | 22        |
| 3  | Photocatalytic reduction of CO2 into CH4 over Ru-doped TiO2: Synergy of Ru and oxygen vacancies.<br>Journal of Colloid and Interface Science, 2022, 608, 2809-2819.   | 9.4  | 63        |
| 4  | Stable and enhanced electrochemical performance based on hierarchical core–shell structure of<br>CoMn <sub>2</sub> O <sub>4</sub> @Ni <sub>3</sub> S <sub>2</sub> electrode for hybrid<br>supercapacitor. Nanotechnology, 2022, 33, 095707.             | 2.6  | 9         |
| 5  | Anchoring RuSe2 on CoSe2 nanoarrays as a hybrid catalyst for efficient and robust oxygen evolution reaction. Journal of Colloid and Interface Science, 2022, 615, 327-334.  | 9.4  | 12        |
| 6  | Nitrogenâ€Doped Bimetallic Carbideâ€Graphite Composite as Highly Active and Extremely Stable<br>Electrocatalyst for Oxygen Reduction Reaction in Alkaline Media. Advanced Functional Materials,<br>2022, 32, .  | 14.9 | 21        |
| 7  | Synergistically Coupled CoMo/CoMoP Electrocatalyst for Highly Efficient and Stable Overall Water<br>Splitting. Inorganic Chemistry, 2022, 61, 8328-8338.  | 4.0  | 26        |
| 8  | Efficient and controllable flame method to generate rich oxygen vacancies in WO <sub>3</sub><br>nanosheet arrays to enhance solar water oxidation. Applied Physics Letters, 2022, 120, 253901.  | 3.3  | 1         |
| 9  | Metal–Organic Framework-Derived Three-Dimensional Macropore Nitrogen-Doped Carbon<br>Frameworks Decorated with Ultrafine Ru-Based Nanoparticles for Overall Water Splitting. Inorganic<br>Chemistry, 2022, 61, 9685-9692.                               | 4.0  | 10        |
| 10 | Regulating photocatalytic CO2 reduction selectivity via steering cascade multi-step charge transfer pathways in 1ÂT/2H-WS2/TiO2 heterojuncitons. Chemical Engineering Journal, 2022, 447, 137485.   | 12.7 | 19        |
| 11 | Ru-doping modulated cobalt phosphide nanoarrays as efficient electrocatalyst for hydrogen evolution rection. Journal of Colloid and Interface Science, 2022, 625, 457-465.  | 9.4  | 27        |
| 12 | A NIRâ€Responsive Phytic Acid Nickel Biomimetic Complex Anchored on Carbon Nitride for Highly<br>Efficient Solar Hydrogen Production. Angewandte Chemie, 2021, 133, 5305-5309.  | 2.0  | 4         |
| 13 | A NIRâ€Responsive Phytic Acid Nickel Biomimetic Complex Anchored on Carbon Nitride for Highly<br>Efficient Solar Hydrogen Production. Angewandte Chemie - International Edition, 2021, 60, 5245-5249.   | 13.8 | 43        |
| 14 | Fe-doped NiCoP/Prussian blue analog hollow nanocubes as an efficient electrocatalyst for oxygen evolution reaction. Electrochimica Acta, 2021, 367, 137492.   | 5.2  | 56        |
| 15 | Integrating Ru-modulated CoP nanosheets binary co-catalyst with 2D g-C3N4 nanosheets for enhanced photocatalytic hydrogen evolution activity. Journal of Colloid and Interface Science, 2021, 585, 108-117.   | 9.4  | 67        |
| 16 | 0D ultrafine ruthenium quantum dot decorated 3D porous graphitic carbon nitride with efficient charge separation and appropriate hydrogen adsorption capacity for superior photocatalytic hydrogen evolution. Dalton Transactions, 2021, 50, 2414-2425. | 3.3  | 13        |
| 17 | Co(OH) <sub>2</sub> water oxidation cocatalyst-decorated CdS nanowires for enhanced photocatalytic CO <sub>2</sub> reduction performance. Dalton Transactions, 2021, 50, 10159-10167.   | 3.3  | 4         |
| 18 | Iron and nitrogen Co-doped CoSe <sub>2</sub> nanosheet arrays for robust electrocatalytic water oxidation. Inorganic Chemistry Frontiers, 2021, 8, 2725-2734.   | 6.0  | 16        |

| #  | Article  | IF   | CITATIONS |
|----|--|------|-----------|
| 19 | Interfacial engineering of CeO <sub>2</sub> on NiCoP nanoarrays for efficient electrocatalytic oxygen evolution. Nanotechnology, 2021, 32, 195704.   | 2.6  | 22        |
| 20 | Accelerating water dissociation kinetic in Co9S8 electrocatalyst by mn/N Co-doping toward efficient alkaline hydrogen evolution. International Journal of Hydrogen Energy, 2021, 46, 7989-8001.  | 7.1  | 23        |
| 21 | Steering Multistep Charge Transfer for Highly Selectively Photocatalytic Reduction of<br>CO <sub>2</sub> into CH <sub>4</sub> over Pd/Cu <sub>2</sub> O/TiO <sub>2</sub> Ternary Hybrid.<br>Solar Rrl, 2021, 5, 2000813.               | 5.8  | 23        |
| 22 | Synergistically Integrating Nickel Porous Nanosheets with 5d Transition Metal Oxides Enabling<br>Efficient Electrocatalytic Overall Water Splitting. Inorganic Chemistry, 2021, 60, 8189-8199.   | 4.0  | 27        |
| 23 | Bimetallic Co-Mo nitride nanosheet arrays as high-performance bifunctional electrocatalysts for overall water splitting. Chemical Engineering Journal, 2021, 411, 128433.  | 12.7 | 143       |
| 24 | Synergistically coupling of Fe-doped CoP nanocubes with CoP nanosheet arrays towards enhanced<br>and robust oxygen evolution electrocatalysis. Journal of Colloid and Interface Science, 2021, 591,<br>67-75.                          | 9.4  | 49        |
| 25 | Interfacial Engineering of the Co <sub><i>x</i></sub> P–Fe <sub>2</sub> P Heterostructure for<br>Efficient and Robust Electrochemical Overall Water Splitting. ACS Sustainable Chemistry and<br>Engineering, 2021, 9, 7737-7748.       | 6.7  | 54        |
| 26 | KCa2Nb3O10/ZnIn2S4 nanosheet heterojunctions with improved charge separation efficiency for efficient photocatalytic CO2 reduction. Journal of Alloys and Compounds, 2021, 865, 158836.  | 5.5  | 27        |
| 27 | Fe-Doped CoP holey nanosheets as bifunctional electrocatalysts for efficient hydrogen and oxygen evolution reactions. International Journal of Hydrogen Energy, 2021, 46, 26391-26401.   | 7.1  | 28        |
| 28 | Synergistic Integration of AuCu Co-Catalyst with Oxygen Vacancies on TiO <sub>2</sub> for Efficient<br>Photocatalytic Conversion of CO <sub>2</sub> to CH <sub>4</sub> . ACS Applied Materials &<br>Interfaces, 2021, 13, 46772-46782. | 8.0  | 65        |
| 29 | Template confined construction of Fe–NiCoP/NiCoP/NF heterostructures for highly efficient<br>electrocatalytic oxygen evolution reaction. International Journal of Hydrogen Energy, 2021, 46,<br>37746-37756.                           | 7.1  | 14        |
| 30 | Synergistic effects of surface Lewis Base/Acid and nitrogen defect in MgAl layered double<br>Oxides/Carbon nitride heterojunction for efficient photoreduction of carbon dioxide. Applied<br>Surface Science, 2021, 563, 150369.       | 6.1  | 26        |
| 31 | Oxygen vacancy engineering of BiOBr/HNb3O8 Z-scheme hybrid photocatalyst for boosting photocatalytic conversion of CO2. Journal of Colloid and Interface Science, 2021, 599, 245-254.  | 9.4  | 49        |
| 32 | Facile synthesis of hierarchical NiCoP nanosheets/NiCoP nanocubes homojunction electrocatalyst<br>for highly efficient and stable hydrogen evolution reaction. Applied Surface Science, 2021, 565, 150537.                             | 6.1  | 33        |
| 33 | Synergistically integrated Co9S8@NiFe-layered double hydroxide core-branch hierarchical architectures as efficient bifunctional electrocatalyst for water splitting. Journal of Colloid and Interface Science, 2021, 604, 680-690.     | 9.4  | 39        |
| 34 | Nickel–manganese bimetallic phosphides porous nanosheet arrays as highly active bifunctional<br>hydrogen and oxygen evolution electrocatalysts for overall water splitting. Electrochimica Acta,<br>2020, 329, 135121.                 | 5.2  | 43        |
| 35 | Covalently Bonded Bi <sub>2</sub> O <sub>3</sub> Nanosheet/Bi <sub>2</sub> WO <sub>6</sub><br>Network Heterostructures for Efficient Photocatalytic CO <sub>2</sub> Reduction. ACS Applied<br>Energy Materials, 2020, 3, 12194-12203.  | 5.1  | 34        |
| 36 | Designing positive electrodes based on 3D hierarchical CoMn <sub>2</sub> O <sub>4</sub> @NiMn-LDH<br>nanoarray composites for high energy and power density supercapacitors. CrystEngComm, 2020, 22,<br>6864-6875.                     | 2.6  | 11        |

| #  | Article  | IF   | CITATIONS |
|----|--|------|-----------|
| 37 | Interfacial engineering of Co3FeN embedded N-doped carbon nanoarray derived from metal–organic<br>frameworks for enhanced oxygen evolution reaction. Electrochimica Acta, 2020, 354, 136629.   | 5.2  | 24        |
| 38 | Holey Cobalt–Iron Nitride Nanosheet Arrays as High-Performance Bifunctional Electrocatalysts for<br>Overall Water Splitting. ACS Applied Materials & Interfaces, 2020, 12, 29253-29263.  | 8.0  | 21        |
| 39 | Hierarchical CoO@Ni(OH) <sub>2</sub> core–shell heterostructure arrays for advanced asymmetric supercapacitors. Nanotechnology, 2020, 31, 405705.  | 2.6  | 17        |
| 40 | Nanowire-assembled Co3O4@NiS core–shell hierarchical with enhanced electrochemical performance for asymmetric supercapacitors. Nanotechnology, 2020, 31, 295403.   | 2.6  | 6         |
| 41 | Synthesis of an iron-doped 3D-ordered mesoporous cobalt phosphide material toward efficient electrocatalytic overall water splitting. Inorganic Chemistry Frontiers, 2020, 7, 3002-3010.   | 6.0  | 22        |
| 42 | Iron-doped nickle cobalt ternary phosphide hyperbranched hierarchical arrays for efficient overall water splitting. Electrochimica Acta, 2020, 334, 135633.  | 5.2  | 38        |
| 43 | Noble-metal-free Co <i> <sub>x</sub> </i> P nanoparticles: modified perovskite oxide ultrathin<br>nanosheet photocatalysts with significantly enhanced photocatalytic hydrogen evolution activity.<br>Nanotechnology, 2020, 31, 325401.      | 2.6  | 2         |
| 44 | MOF-derived cobalt oxides nanoparticles anchored on CoMoO4 as a highly active electrocatalyst for oxygen evolution reaction. Journal of Alloys and Compounds, 2019, 806, 1097-1104.  | 5.5  | 41        |
| 45 | Integration of ZnCo2S4 nanowires arrays with NiFe-LDH nanosheet as water dissociation promoter for enhanced electrocatalytic hydrogen evolution. Electrochimica Acta, 2019, 324, 134861.   | 5.2  | 26        |
| 46 | Hierarchically structured Co3O4@glucose-modified LDH architectures for high-performance supercapacitors. Applied Surface Science, 2019, 488, 639-647.  | 6.1  | 40        |
| 47 | Synergistic coupling of CoFe-LDH arrays with NiFe-LDH nanosheet for highly efficient overall water splitting in alkaline media. Applied Catalysis B: Environmental, 2019, 253, 131-139.  | 20.2 | 503       |
| 48 | Hierarchical urchin-like Co <sub>9</sub> S <sub>8</sub> @Ni(OH) <sub>2</sub> heterostructures with<br>superior electrochemical performance for hybrid supercapacitors. New Journal of Chemistry, 2019, 43,<br>8444-8451.                     | 2.8  | 14        |
| 49 | CoP <sub>3</sub> /CoMoP Heterogeneous Nanosheet Arrays as Robust Electrocatalyst for pH-Universal<br>Hydrogen Evolution Reaction. ACS Sustainable Chemistry and Engineering, 2019, 7, 9309-9317.   | 6.7  | 97        |
| 50 | Coupling Co2P and CoP nanoparticles with copper ions incorporated Co9S8 nanowire arrays for<br>synergistically boosting hydrogen evolution reaction electrocatalysis. Journal of Colloid and<br>Interface Science, 2019, 550, 10-16.         | 9.4  | 47        |
| 51 | MoS2/SnNb2O6 2D/2D nanosheet heterojunctions with enhanced interfacial charge separation for boosting photocatalytic hydrogen evolution. Journal of Colloid and Interface Science, 2019, 536, 1-8.   | 9.4  | 60        |
| 52 | Syntheses, Crystal Structures, and Properties of Three Novel Silver–Organic Frameworks Assembled<br>from 1,2,3,5-Benzenetetracarboxylic Acid Based on Argentophilic Interactions. Crystal Growth and<br>Design, 2018, 18, 1978-1986.         | 3.0  | 16        |
| 53 | Construction of RGO/CdIn 2 S 4 /g-C 3 N 4 ternary hybrid with enhanced photocatalytic activity for the degradation of tetracycline hydrochloride. Applied Surface Science, 2018, 433, 388-397.   | 6.1  | 91        |
| 54 | Enhanced photocatalytic activity of graphitic carbon nitride/carbon nanotube/Bi2WO6 ternary<br>Z-scheme heterojunction with carbon nanotube as efficient electron mediator. Journal of Colloid<br>and Interface Science, 2018, 512, 693-700. | 9.4  | 101       |

| #  | Article   | IF   | CITATIONS |
|----|---|------|-----------|
| 55 | Grapheneâ€5ensitized Perovskite Oxide Monolayer Nanosheets for Efficient Photocatalytic Reaction.<br>Advanced Functional Materials, 2018, 28, 1806284.  | 14.9 | 48        |
| 56 | Construction of Novel CdS/SnNb2 O6 Heterojunctions with Enhanced Photocatalytic Degradation<br>Activity Under Visible Light. European Journal of Inorganic Chemistry, 2018, 2018, 4812-4818.  | 2.0  | 6         |
| 57 | Engineering Ni(OH) <sub>2</sub> Nanosheet on CoMoO <sub>4</sub> Nanoplate Array as Efficient<br>Electrocatalyst for Oxygen Evolution Reaction. ACS Sustainable Chemistry and Engineering, 2018, 6,<br>16086-16095.  | 6.7  | 64        |
| 58 | Construction of novel Sr0.4H1.2Nb2O6·H2O/g-C3N4 heterojunction with enhanced visible light photocatalytic activity for hydrogen evolution. Journal of Colloid and Interface Science, 2018, 526, 451-458.  | 9.4  | 26        |
| 59 | Dion–Jacobson-type perovskite KCa <sub>2</sub> Ta <sub>3</sub> O <sub>10</sub> nanosheets hybridized<br>with g-C <sub>3</sub> N <sub>4</sub> nanosheets for photocatalytic H <sub>2</sub> production.<br>Catalysis Science and Technology, 2018, 8, 3767-3773.  | 4.1  | 26        |
| 60 | CdS nanoparticles decorated K+Ca2Nb3O10â^' nanosheets with enhanced photocatalytic activity.<br>Materials Letters, 2018, 229, 236-239.  | 2.6  | 7         |
| 61 | Assembly of WO3 nanosheets/Bi24O31Br10 nanosheets composites with superior photocatalytic activity for degradation of tetracycline hydrochloride. Journal of Materials Science, 2018, 53, 15804-15816.  | 3.7  | 14        |
| 62 | Synthesis and electrochemical performance of LiFePO4/C cathode materials from Fe2O3 for high-power lithium-ion batteries. Ionics, 2017, 23, 377-384.  | 2.4  | 8         |
| 63 | Construction of ultrafine TiO <sub>2</sub> nanoparticle and SnNb <sub>2</sub> O <sub>6</sub><br>nanosheet 0D/2D heterojunctions with abundant interfaces and significantly improved photocatalytic<br>activity. Catalysis Science and Technology, 2017, 7, 2308-2317.                                     | 4.1  | 39        |
| 64 | CdIn <sub>2</sub> S <sub>4</sub> /g-C <sub>3</sub> N <sub>4</sub> heterojunction photocatalysts:<br>enhanced photocatalytic performance and charge transfer mechanism. RSC Advances, 2017, 7, 231-237.  | 3.6  | 52        |
| 65 | SrTiO <sub>3</sub> Nanoparticle/SnNb <sub>2</sub> O <sub>6</sub> Nanosheet 0D/2D Heterojunctions<br>with Enhanced Interfacial Charge Separation and Photocatalytic Hydrogen Evolution Activity. ACS<br>Sustainable Chemistry and Engineering, 2017, 5, 9749-9757.   | 6.7  | 54        |
| 66 | RGO-Promoted All-Solid-State g-C <sub>3</sub> N <sub>4</sub> /BiVO <sub>4</sub> Z-Scheme<br>Heterostructure with Enhanced Photocatalytic Activity toward the Degradation of Antibiotics.<br>Industrial & Engineering Chemistry Research, 2017, 56, 8823-8832.   | 3.7  | 116       |
| 67 | Construction of novel WO3/SnNb2O6 hybrid nanosheet heterojunctions as efficient Z-scheme photocatalysts for pollutant degradation. Journal of Colloid and Interface Science, 2017, 506, 93-101.   | 9.4  | 57        |
| 68 | 2D/2D heterojunctions of WO <sub>3</sub><br>nanosheet/K <sup>+</sup> Ca <sub>2</sub> Nb <sub>3</sub> O <sub>10</sub> <sup>â^'</sup> ultrathin<br>nanosheet with improved charge separation efficiency for significantly boosting photocatalysis.<br>Catalysis Science and Technology, 2017, 7, 3481-3491. | 4.1  | 68        |
| 69 | Perovskite oxide ultrathin nanosheets/g-C3N4 2D-2D heterojunction photocatalysts with significantly enhanced photocatalytic activity towards the photodegradation of tetracycline. Applied Catalysis B: Environmental, 2017, 201, 617-628.  | 20.2 | 360       |
| 70 | Enhancement of g-C 3 N 4 nanosheets photocatalysis by synergistic interaction of ZnS microsphere<br>and RGO inducing multistep charge transfer. Applied Catalysis B: Environmental, 2016, 198, 200-210.   | 20.2 | 165       |
| 71 | Synthesis, characterization, and adsorption properties of silica aerogels crosslinked with diisocyanate under ambient drying. Journal of Materials Science, 2016, 51, 9472-9483.  | 3.7  | 15        |
| 72 | Ag nanoparticle-decorated CoS nanosheet nanocomposites: a high-performance material for<br>multifunctional applications in photocatalysis and supercapacitors. RSC Advances, 2016, 6,<br>55039-55045.   | 3.6  | 36        |

| #  | Article   | IF   | CITATIONS |
|----|---|------|-----------|
| 73 | Synthesis of cuprous oxide with morphological evolution from truncated octahedral to spherical structures and their size and shape-dependent photocatalytic activities. Journal of Colloid and Interface Science, 2016, 461, 25-31.   | 9.4  | 26        |
| 74 | In-situ synthesis and enhanced photocatalytic activity of visible-light-driven plasmonic<br>Ag/AgCl/NaTaO3 nanocubes photocatalysts. Applied Catalysis B: Environmental, 2016, 191, 228-234.  | 20.2 | 126       |
| 75 | Novel β-In <sub>2.77</sub> S <sub>4</sub> nanosheet-assembled hierarchical microspheres: synthesis and high performance for photocatalytic reduction of Cr( <scp>vi</scp> ). RSC Advances, 2016, 6, 18227-18234.  | 3.6  | 14        |
| 76 | Construction of SnNb 2 O 6 nanosheet/g-C 3 N 4 nanosheet two-dimensional heterostructures with improved photocatalytic activity: Synergistic effect and mechanism insight. Applied Catalysis B: Environmental, 2016, 183, 113-123.  | 20.2 | 239       |
| 77 | Synthesis, Crystal Structure, Fluorescence and Photocatalytic Properties of a Copper Compound with<br>2â€Phenylâ€1Hâ€1,3,7,8â€tetraazacyclopenta[l]phenanthrene and Silicotungstic Acid. Zeitschrift Fur<br>Anorganische Und Allgemeine Chemie, 2015, 641, 826-830.                       | 1.2  | 2         |
| 78 | Two-Dimensional Caln <sub>2</sub> S <sub>4</sub> /g-C <sub>3</sub> N <sub>4</sub> Heterojunction<br>Nanocomposite with Enhanced Visible-Light Photocatalytic Activities: Interfacial Engineering and<br>Mechanism Insight. ACS Applied Materials & Interfaces, 2015, 7, 19234-19242.      | 8.0  | 307       |
| 79 | Angstrom-scale vanadium carbide rods as Pt electrocatalyst support for efficient methanol oxidation reaction. RSC Advances, 2015, 5, 9561-9564.   | 3.6  | 7         |
| 80 | Fabrication of a Ag/Bi <sub>3</sub> TaO <sub>7</sub> Plasmonic Photocatalyst with Enhanced<br>Photocatalytic Activity for Degradation of Tetracycline. ACS Applied Materials & Interfaces, 2015,<br>7, 17061-17069.   | 8.0  | 251       |
| 81 | Controllable synthesis of fluorapatite microcrystals decorated with silver nanoparticles and their optical properties. RSC Advances, 2015, 5, 12392-12396.  | 3.6  | 11        |
| 82 | Synthesis and size-dependent electrochemical nonenzymatic H2O2 sensing of cuprous oxide nanocubes. RSC Advances, 2015, 5, 82496-82502.  | 3.6  | 21        |
| 83 | A g-C <sub>3</sub> N <sub>4</sub> /nanocarbon/Znln <sub>2</sub> S <sub>4</sub> nanocomposite: an<br>artificial Z-scheme visible-light photocatalytic system using nanocarbon as the electron mediator.<br>Chemical Communications, 2015, 51, 17144-17147.                                 | 4.1  | 136       |
| 84 | Natural carbon nanodots assisted development of size-tunable metal (Pd, Ag) nanoparticles grafted<br>on bionic dendritic α-Fe <sub>2</sub> O <sub>3</sub> for cooperative catalytic applications. Journal of<br>Materials Chemistry A, 2015, 3, 23607-23620.                              | 10.3 | 39        |
| 85 | Ag-Decorated ATaO <sub>3</sub> (A = K, Na) Nanocube Plasmonic Photocatalysts with Enhanced<br>Photocatalytic Water-Splitting Properties. Langmuir, 2015, 31, 9694-9699.   | 3.5  | 71        |
| 86 | ZnS microsphere/g-C <sub>3</sub> N <sub>4</sub> nanocomposite photo-catalyst with greatly enhanced visible light performance for hydrogen evolution: synthesis and synergistic mechanism study. RSC Advances, 2014, 4, 62223-62229.   | 3.6  | 46        |
| 87 | N-doped graphene quantum dots as an effective photocatalyst for the photochemical synthesis of silver deposited porous graphitic C <sub>3</sub> N <sub>4</sub> nanocomposites for nonenzymatic electrochemical H <sub>2</sub> O <sub>2</sub> sensing. RSC Advances, 2014, 4, 16163-16171. | 3.6  | 72        |
| 88 | Highly efficient heterojunction photocatalyst based on nanoporous g-C3N4 sheets modified by Ag3PO4<br>nanoparticles: Synthesis and enhanced photocatalytic activity. Journal of Colloid and Interface<br>Science, 2014, 417, 115-120.   | 9.4  | 143       |
| 89 | In situ synthesis of bimetallic Ag/Pt loaded single-crystalline anatase TiO2 hollow nano-hemispheres and their improved photocatalytic properties. CrystEngComm, 2014, 16, 2384.  | 2.6  | 64        |
| 90 | MoC–graphite composite as a Pt electrocatalyst support for highly active methanol oxidation and oxygen reduction reaction. Journal of Materials Chemistry A, 2014, 2, 4014.   | 10.3 | 106       |

| #   | Article  | IF   | CITATIONS |
|-----|--|------|-----------|
| 91  | Hydrothermal synthesis of In 2 S 3 /g-C 3 N 4 heterojunctions with enhanced photocatalytic activity.<br>Journal of Colloid and Interface Science, 2014, 433, 9-15.   | 9.4  | 159       |
| 92  | The synthesis of a novel Ag–NaTaO3 hybrid with plasmonic photocatalytic activity under visible-light.<br>CrystEngComm, 2014, 16, 1384.   | 2.6  | 31        |
| 93  | One-pot synthesis of 1-acetylpyrene over supported phosphotungstic heteropoly acid catalysts.<br>Reaction Kinetics, Mechanisms and Catalysis, 2013, 108, 531-544.  | 1.7  | 4         |
| 94  | Small-sized Pt particles on mesoporous hollow carbon spheres for highly stable oxygen reduction reaction. Electrochimica Acta, 2013, 109, 256-261.   | 5.2  | 27        |
| 95  | Facile synthesis of core–shell–satellite Ag/C/Ag nanocomposites using carbon nanodots as reductant<br>and their SERS properties. CrystEngComm, 2013, 15, 6305.   | 2.6  | 24        |
| 96  | In-situ ion exchange synthesis of hierarchical Agl/BiOI microsphere photocatalyst with enhanced photocatalytic properties. CrystEngComm, 2013, 15, 7556.   | 2.6  | 100       |
| 97  | Natural leaves-assisted synthesis of nitrogen-doped, carbon-rich nanodots-sensitized, Ag-loaded<br>anatase TiO2 square nanosheets with dominant {001} facets and their enhanced catalytic applications.<br>Journal of Materials Chemistry A, 2013, 1, 14963. | 10.3 | 69        |
| 98  | Efficient Synthesis of 1-Acetylpyrene Using [Bmim]Cl–FeCl3 Ionic Liquid as Dual Catalyst and Solvent.<br>International Journal of Chemical Reactor Engineering, 2013, 11, 1-7.   | 1.1  | 58        |
| 99  | Modifiers-assisted formation of nickel nanoparticles and their catalytic application to p-nitrophenol reduction. CrystEngComm, 2013, 15, 560-569.  | 2.6  | 244       |
| 100 | Novel p–n heterojunction photocatalyst constructed by porous graphite-like C3N4 and<br>nanostructured BiOI: facile synthesis and enhanced photocatalytic activity. Dalton Transactions, 2013,<br>42, 15726.  | 3.3  | 333       |
| 101 | Facile synthesis and characterisation of hexagonal magnetite nanoplates. Micro and Nano Letters, 2013, 8, 383-385.   | 1.3  | 12        |
| 102 | Facile route fabrication of nano-Ni core mesoporous-silica shell particles with high catalytic activity towards 4-nitrophenol reduction. CrystEngComm, 2012, 14, 4601.   | 2.6  | 109       |
| 103 | Synthesis of 1-benzoylpyrene using silica-supported phosphotungstic heteropoly acid as an efficient and reusable catalyst. Korean Journal of Chemical Engineering, 2012, 29, 1388-1392.  | 2.7  | 4         |
| 104 | Photoenhanced degradation of rhodamine blue on monometallic gold (Au) loaded brookite titania<br>photocatalysts activated by visible light. Reaction Kinetics, Mechanisms and Catalysis, 2012, 107,<br>487-502.  | 1.7  | 11        |
| 105 | One-pot synthesis of 5-acetylacenaphthene using heteropoly acid catalysts. Reaction Kinetics,<br>Mechanisms and Catalysis, 2011, 102, 103-111.   | 1.7  | 6         |
| 106 | Novel Countercation in MMX-Type Mixed-Valence Chain Compound: Coexistence of Neutral and Protonated Amino Substituents. Polymers, 2011, 3, 1652-1661.  | 4.5  | 6         |
| 107 | Preparation and characterization of heterojunction semiconductor<br>YFeO <sub>3</sub> /TiO <sub>2</sub> with an enhanced photocatalytic activity. Journal of Materials<br>Research, 2010, 25, 104-109.   | 2.6  | 16        |
| 108 | Poly[[μ2-1,2-bis(imidazol-1-ylmethyl)benzene](μ2-cyclohexane-1,4-dicarboxylato)cobalt(II)]. Acta<br>Crystallographica Section E: Structure Reports Online, 2010, 66, m330-m330.  | 0.2  | 0         |

| #   | Article   | IF  | CITATIONS |
|-----|---|-----|-----------|
| 109 | Alkylation of anthracene to 2-isopropylanthracene catalyzed by Lewis acid ionic liquids. Korean<br>Journal of Chemical Engineering, 2009, 26, 1563-1567.                        | 2.7 | 19        |
| 110 | Preparation of 3,6-dibenzoylacenapthene in the presence of Lewis acidic ionic liquids. Reaction<br>Kinetics and Catalysis Letters, 2009, 98, 355-363.                           | 0.6 | 10        |
| 111 | Comparative effects of five chelating agents on testicular toxicity in mice induced by acute exposure to cadmium. Toxicological and Environmental Chemistry, 2006, 88, 325-330. | 1.2 | 1         |